OXFORD JLB JOURNAL OF LEUKOCYTE BIOLOGY

*Journal of Leukocyte Biology*, 2023, **00**, 1–12

https://doi.org/10.1093/jleuko/qiad123

**Meeting Article**

# The invasive margin of early-stage human colon tumors is infiltrated with neutrophils of an antitumoral phenotype

Eduardo Vadillo,[1,*] Alejandra Mantilla,[2] Cristina Aguilar-Flores,[3] Saraí Gisel De León-Rodríguez,[4] Sandra Vela-Patiño,[5] Juan Badillo,[1] Keiko Taniguchi-Ponciano,[5] Daniel Marrero-Rodríguez,[5] Lourdes Ramírez,[6] Iliana Itzel León-Vega,[7] Carmen Fuentes-Castañeda,[1] Patricia Piña-Sánchez,[1] Jessica Lakshmi Prieto-Chávez,[8] Vadim Pérez-Kondelkova,[9] Juan José Montesinos,[1] Laura Bonifaz,[4,10] Rosana Pelayo,[11,12] Héctor Mayani,[1] and Michael Schnoor[7]

[1]Unidad de Investigación Médica en Enfermedades Oncológicas, UMAE Hospital de Oncología, Centro Médico Nacional Siglo XXI, Instituto Mexicano del Seguro Social (CMN S.XXI IMSS), Avenida Cuauhtémoc No. 330, Colonia Doctores, Mexico City 06720, Mexico
[2]Servicio de Patología, Hospital de Oncología CMN S.XXI IMSS, Avenida Cuauhtémoc No. 330, Colonia Doctores, Mexico City 06720, Mexico
[3]UMAE Hospital de Pediatría, CMN S.XXI IMSS, Avenida Cuauhtémoc No. 330, Colonia Doctores, Mexico City 06720, Mexico
[4]Unidad de Investigación Médica en Inmunoquímica, UMAE Hospital de Especialidades, CMN S.XXI IMSS, Avenida Cuauhtémoc No. 330, Colonia Doctores, Mexico City 06720, Mexico
[5]Unidad de Investigación Médica en Enfermedades Endocrinas, UMAE Hospital de Especialidades, CMN S.XXI IMSS, Avenida Cuauhtémoc No. 330, Colonia Doctores, Mexico City 06720, Mexico
[6]Servicio de Colon y Recto, Hospital de Oncología CMN S.XXI IMSS, Avenida Cuauhtémoc No. 330, Colonia Doctores, Mexico City 06720, Mexico
[7]Departmento de Biomedicina Molecular, CINVESTAV-IPN, Av. IPN 2508, San Pedro Zacatenco, Mexico City 07360, Mexico
[8]Laboratorio de Citometría—Centro de Instrumentos, División de Desarrollo de la Investigación en Salud, CMN S.XXI IMSS, Av Cuauhtémoc No. 330, Colonia Doctores, Mexico City 06720, Mexico
[9]Laboratorio Nacional de Microscopía Avanzada, División de Desarrollo de la Investigación, CMN S.XXI IMSS, Avenida Cuauhtémoc No. 330, Colonia Doctores, Mexico City 06720, Mexico
[10]Coordinación de Investigación en Salud, CMN S.XXI IMSS, Avenida Cuauhtémoc No. 330, Colonia Doctores, Mexico City 06720, Mexico
[11]Unidad de Educación e Investigación, IMSS, Avenida Cuauhtémoc No. 330, Colonia Doctores, Mexico City 06720, Mexico
[12]Centro de Investigación Biomédica de Oriente, IMSS, Km 4.5 Carretera Atlixco-Metepec, Atlixco-Metepec, 74360 Puebla, Mexico
*Corresponding author: Unidad de Investigación Médica en Enfermedades Oncológicas, UMAE Hospital de Oncología, Centro Médico Nacional Siglo XXI, Instituto Mexicano del Seguro Social (CMN S.XXI IMSS), Avenida Cuauhtémoc No.330, Colonia Doctores, Mexico City 06720, Mexico. Email: evadillo@hotmail.com or eduardo.vadillo@imss.gob.mx

## Abstract

Neutrophils infiltrate several types of cancer; however, whether their presence is associated with disease progression remains controversial. Here, we show that colon tumors overexpress neutrophil chemoattractants compared to healthy tissues, leading to their recruitment to the invasive margin and the central part of colon tumors. Of note, tumor-associated neutrophils expressing tumor necrosis factor α, which usually represents an antitumoral phenotype, were predominantly located in the invasive margin. Tumor-associated neutrophils from the invasive margin displayed an antitumoral phenotype with higher ICAM-1 and CD95 expression than neutrophils from healthy adjacent tissues. A higher neutrophil/lymphocyte ratio was found at later stages compared to the early phases of colon cancer. A neutrophil/lymphocyte ratio ≤3.5 predicted tumor samples had significantly more neutrophils at the invasive margin and the central part. Moreover, tumor-associated neutrophils at the invasive margin of early-stage tumors showed higher ICAM-1 and CD95 expression. Coculture of colon cancer cell lines with primary neutrophils induced ICAM-1 and CD95 expression, confirming our in situ findings. Thus, our data demonstrate that tumor-associated neutrophils with an antitumoral phenotype characterized by high ICAM-1 and CD95 expression infiltrate the invasive margin of early-stage colon tumors, suggesting that these cells can combat the disease at its early courses. The presence of tumor-associated neutrophils with antitumoral phenotype could help predict outcomes of patients with colon cancer.

**Keywords:** CD95, CXCR2, ICAM-1, cancer progression, polarization

## 1. Introduction

Colorectal cancer (CRC) is the third most common type of cancer and the second leading cause of mortality worldwide. In 2020, 147,950 new cases of CRC were expected in the United States, of which 104,610 correspond to colon cancer and 43,340 correspond to rectal cancer.[1] Surgical resection of both primary lesions[2] and metastases[3] is the best option for these patients; however, recurrence, which occurs in approximately 68% of patients, complicates their outcome.[4–6]

The evolution of the disease starts from an epithelium that presents a high proliferative capacity. This capacity can lead to focal dysplastic crypt formation, generating a macroscopic tubular or villous adenoma that progresses to a high-grade dysplasia; the last stage of primary tumor formation in CRC comprises the generation of invasive carcinoma. The malignant potential of a

**Received:** April 15, 2023. **Revised:** September 13, 2023. **Accepted:** September 18, 2023

tumor, its progression, and metastasis partially depend on the cells that form the tumor microenvironment (TME), including endothelial cells, mesenchymal stromal cells, and leukocytes.[7] The lineage and number of leukocytes infiltrating a tumor and their disposition within the TME determine a prognostic risk factor for patients with different neoplasms.[8] For example, macrophage polarization within tumors toward phenotypes that promote tumor progression is an infallible strategy for the immune evasion of cancer cells.[7]

To date, there is controversy about the role of neutrophils in CRC. It is known from mice single-cell RNA sequencing (RNA-seq) experiments that neutrophils are comprehended by 8 different populations.[9] The proportion of these populations is influenced by their state of maturation, aging, tissue location, and consequent activation state, all affecting phenotype and functional characteristics.[10] In humans and mice, inflammatory mediators such as lipopolysaccharide or interferons are capable of inducing a proinflammatory phenotype of neutrophils (N1) while transforming growth factor β (TGFβ), interleukin (IL) 10, and prostaglandin E2 can induce an anti-inflammatory phenotype.[11–13] Moreover, polymorphonuclear (PMN)–derived myeloid-derived suppressor cells, which are mostly immature, are generated during cancer and other diseases to exert immunosuppressive features.[14] However, it is difficult to trace them because cell surface markers overlap with other neutrophil populations.[15] Neutrophils and macrophages can modify their phenotype and function depending on the context in which they are found.[10] Previous work has demonstrated that high numbers of neutrophils in CRC correlate with a worse prognosis.[16] However, more recent reports have shown that tumor-associated neutrophils (TANs) confer better survival in patients with CRC.[17,18] Moreover, TANs in CRC locate in both the central zone of the tumor (CT) and the invasive margin (IM) at similar proportions where they interact with both tumoral and stromal cells.[19–21] Despite this discovery, their phenotypes and functions in these tumor zones remain unknown.

Most information concerning the role of neutrophils in cancer comes from murine models. For example, in a mouse mesothelioma model, stimulation with TGFβ polarizes neutrophils toward a protumoral phenotype (with the ability to produce CCL2, CCL5, and arginase). Upon TGFβ receptor inhibition, neutrophils acquire antitumoral characteristics by producing tumor necrosis factor α (TNFα) and expressing intercellular adhesion molecule 1 (ICAM-1) and apoptosis antigen 1 (FAS/CD95).[12] In mouse melanoma and breast cancer models, interferon-β (IFN-β) induces ICAM-1, CD95, and TNFα expression in neutrophils, a phenotype associated with antitumoral properties.[22] In the absence of IFN-β, the growth of a fibrosarcoma was promoted by neutrophils expressing CXCR4, Vascular Endothelial Growth Factor, and Matrix Metalloproteinase 9.[23]

Neutrophils produce a variety of inflammatory mediators in response to tumor-dependent stimuli. For example, neutrophil elastase contributes to lung cancer progression in mice by inducing tumor cell proliferation.[24] By contrast, chemokines that neutrophils secreted in the context of lung cancer, including CCL-2, CCL-3, CXCL-8, and IL-6, promoted an antitumoral environment by enhancing T-cell functions.[25] Tumor-derived chemokines, including CXCL8, are recognized by CXCR2 in human neutrophils to promote the progression of pancreatic and lung cancer in murine models.[26] However, whether the presence of neutrophils in different layers of the tumor and their characteristics could be associated with disease progression remains elusive. Therefore, we hypothesized that the frequency and phenotype of TANs is related to disease progression in colon cancer.

## 2. Methods

### 2.1 In silico transcriptome analysis

For transcriptome analysis, 231 normal and 342 colon cancer tissue samples were selected. The data used for these analyses were downloaded from European Bioinformatics Institute and Gene Expression Omnibus. These data correspond to GSE4183, GSE8671, GSE9348, GSE15960, GSE20916, GSE21510, GSE22598, GSE23194, GSE23878, GSE32323, GSE33113, and GSE37364. Data set analyses were achieved using CEL files with the Transcriptome Analysis Console (Affymetrix). Pearson and Spearman correlation was performed and probe sets were summarized through median polish and normalized by quantiles with no probe sets excluded from the analysis. Background noise correction was achieved by means of robust multichip average, and data were $\log_2$-transformed. Data grouping and categorization were achieved by principal component analysis. Differentially expressed genes were detected through analysis of variance. Genes were considered altered with +2- or −2-fold change, $P \leq 0.01$, and False Discovery Rate > 0.01 parameters. Data obtained from the abovementioned analysis were corroborated with analysis at the GEPIA platform.[27,28]

### 2.2 Deconvolution analysis

The deconvolution analysis was performed using the online tool CIBERSORT (Cell Type Identification By Estimating Relative Samples Of RNA Transcripts), which solves the equation $m = f \times B$, where m is a mixture of messenger RNA (mRNA), f is a vector that denotes the cell fractions that make up the mixture, and B is an array of gene expression profiles characteristic of each cell subtype. CIBERSORT is based on the application of v-SVR (nu-support vector regression), where limits of a hyperplane are determined that fits most of the possible points at a constant distance and where a regression is performed. Support vectors are genes selected from B. CIBERSORT was used for the present work with the default parameters, using the LM22 expression profile matrix (22 types of immune cells) and 100 permutations to calculate the P value associated by Monte Carlo sampling. The mRNA mixture was a matrix constructed with the expression values of each sample obtained by microarrays.

### 2.3 Patient samples

The Mexican Institute for Social Security National Ethics Committee approved all methods (R-2022-785-048). All patients received treatment at the Oncology Hospital at the National Medical Center, Mexican Institute of Social Security (IMSS). All patients agreed to participate in the study, and in accordance with the Declaration of Helsinki, written informed consent was provided. A portion of 1 $cm^3$ from healthy adjacent tissue (HAT),[29] the CT, and the IM of the tumor was included in paraffin and analyzed by expert pathologists.[21] A complementary 1 $cm^3$ fresh portion of the tumor and control tissue was immediately processed by flow cytometry analysis. All samples included in the study were diagnosed as adenocarcinomas from the colon's ascending, transverse, or sigmoid portions. All patient characteristics are included in Supplementary Table 1.

### 2.4 Histopathology

Paraffin blocks were cut at a thickness of 4-μm sections in a Leica RM 2125. Hematoxylin and eosin (H&E) staining was performed

according to standard protocols to confirm a colon cancer diagnosis.

### 2.5 Whole-tissue scanning

Complete colon cancer H&E images were obtained with an Aperio CS2 Leica 20× (Leica Biosystems). The exported regions of interest were extracted with eSlide Scan Scope v12.3.3.

### 2.6 Tissue embedding and immunofluorescence staining

Resection paraffined products were cut in sections of 3 μm with a microtome and mounted on electro-charged glass slides (Kling-On HIER Slides). Slides were placed into an oven (70 °C) for 45 min and then tissues were rehydrated with a xylol/ethanol train of solvents. A citrate buffer pH 6.0 (sodium citrate 10 μM) was used to perform antigen retrieval (90 °C for 20 min). Samples were permeabilized with 0.3% Triton for 2 h. Following permeabilization, samples were incubated with anti-CD66b (PE, BioLegend, 392904), anti-TNFα (AF488, Biolegend, 502915), and anti-CD11b (purified, Abcam ab133357). The purified antibody was revealed with a secondary conjugated antibody anti-rabbit Alexa Fluor 647 (Jackson Immunoresearch 711-605-152). After that, nuclei were counterstained with Hoechst (Invitrogen) for 10 min. Sections were mounted with Vecta-Shield (Vector, H-1000). Images were acquired after this step of staining and used for analysis. Samples were acquired as described below. Using the H&E scans, 3 highly infiltrated areas in the HAT, CT, or IM were chosen to assess the specified phenotype of the cells.

### 2.7 Confocal microscopy

Micrographs were obtained on a Nikon Ti Eclipse inverted confocal microscope (Nikon Corporation) using NIS Elements v.4.50. Imaging was performed using a 20× (dry, NA 0.75) objective lens. During image acquisition, additional magnification (3.4×) was attained through Nyquist sampling. Three areas of high infiltrate from each group were taken to quantify the percentage and density of neutrophil cells.

### 2.8 Immunofluorescence image analysis

Immunofluorescence analyses were performed using our machine learning method described in De León Rodríguez et al.[30] Briefly, this method is based on the segmentation of nuclei in order to phenotype each cell accordingly to the expression of different markers. To perform the segmentation, we used our trained model in Cellpose, a deep neural network with U-Net architecture.[31] Subsequently, we used machine learning–trained classifiers in Annotater ImageJ.[32] The results obtained were analyzed using Python scripts. The percentage of positive cells was calculated by dividing the total number of cells positive for a given phenotype by the total number of cells in the field multiplied by 100. The density was measured by dividing the number of cells of interest by the total area of the field. The mean fluorescence intensity was normalized and transformed to a logarithmic scale. The results shown represent the media value of 3 analyzed areas per patient. Only marks with nuclei were analyzed.

### 2.9 Tumor digestion

Tumors were digested as previously described.[33] Briefly, fresh tumor samples were washed with an isotonic saline solution. Tissues were placed in 24-well plates and minced in a digestion solution containing 1 mg/mL collagenase and 100 U/mL hyaluronidase. Preparation was incubated at 37 °C at 300 rpm for 30 min (Thermomixer C, Eppendorf). Then, the cell suspension was macerated and filtered through a 70 μm mesh. The cells were washed with a staining buffer before flow cytometry staining.

### 2.10 Flow cytometry

In total, $1 \times 10^6$ cells from the digested cell suspension were simultaneously blocked and stained with the following antibodies: anti-human (CD45-AF647, CD66b-PE, CD11a-AF488, CXCR2-PB, Mac-1 PB, CD62L-AF488, CD95-PB, CD162-PE, and CD54-PB), all from Biolegend. 7-AAD was used as a dead cell discriminator. Unstained cells derived from each digested tumor section were used to define the expression of each marker. After 30 min of incubation at room temperature, all preparations were extensively washed with Fluorescense-Activated Cell Sorting solution. All preparations were fixed with paraformaldehyde 2% for 15 min. Cells were washed and acquired in a Cytek Northern Lights Spectral cytometer. Acquired data were analyzed with FlowJo VX software.

### 2.11 Neutrophil isolation

Healthy peripheral blood donors were phlebotomized using the Vacutainer system (BD Biosciences). Blood was anticoagulated with EDTA. Blood was diluted with phosphate-buffered saline (PBS) 1× and submitted to gradient separation employing the Histopaque 1.077 g/L and 1.119 g/L (Sigma) according to the manufacturer's specifications. Briefly, the preparation was centrifugated at 800 *g* for 30 min. PMN cells were collected, washed twice, counted, and resuspended with the desired supplemented cell culture media.

### 2.12 Coculture systems

CaCo2 and HCT116 cell lines were grown with 10% fetal calf serum (FCS)–supplemented Dulbecco's modified Eagle's medium F12 culture media. Both cell lines were cultured up to 90% confluency in 24-well plates. After PMN isolation, $2 \times 10^6$ cells were cocultured for 48 h in the presence of tumoral cells. As controls, neutrophils were cultured in the absence of tumoral cells under the same conditions. To avoid PMN activation, cells were cocultured with media supplemented at 3% FCS. Media were supplemented with the apoptosis inhibitor QVD-Oph (Sigma Aldrich) at 3 μM.[29] Cells were then harvested with vensene, counted, and prepared for flow cytometry analysis, as previously mentioned.

### 2.13 Neutrophil/lymphocyte ratio

The neutrophil/lymphocyte (NLR) was calculated from preoperative laboratory studies. The NLR was calculated by dividing absolute neutrophil counts between absolute lymphocyte counts. White blood cell counts were performed automatically in a cell counter (Sysmex). A threshold of 3.5 was established based on previous publications[34] and calculated by generating a receiver operator characteristic curve with the SPSS Statistics (IBM) program.

### 2.14 Statistics

Data were analyzed using GraphPad Prism Version 8.0 (GraphPad Software). Student's *t* test was employed to compare the mean and SD among groups. *P* values $<0.05$ were considered statistically significant.

## 3. Results

### 3.1 Colon cancer tumors overexpress transcripts related to molecules involved in neutrophil recruitment

Tumors produce a plethora of molecules to influence the microenvironment they occupy. Thus, we first investigated which

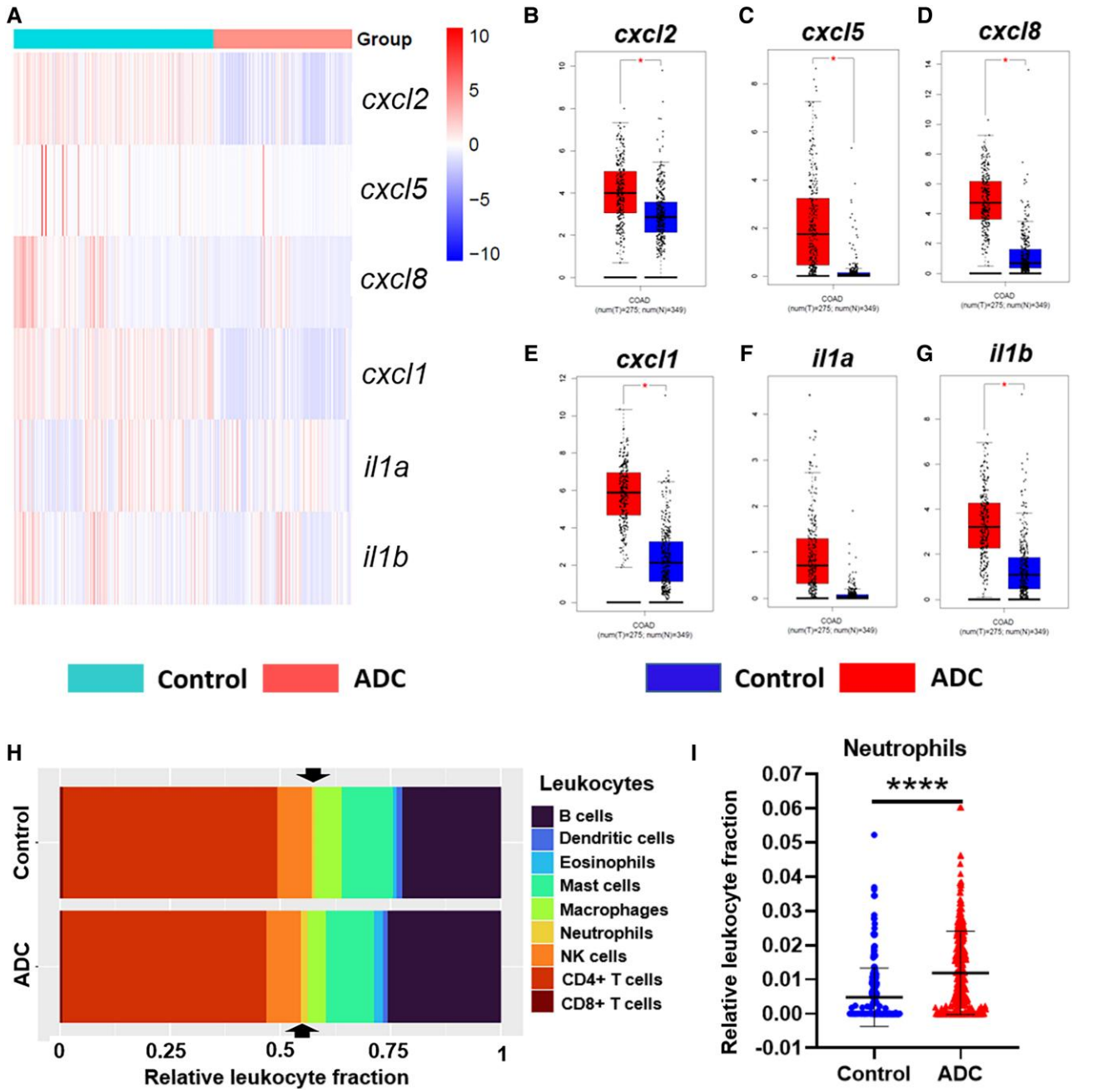


Fig. 1. Colon cancer tumors overexpress transcripts related to molecules involved in neutrophil recruitment. (A) Supervised analysis of ADC vs control data sets regarding the expression of *cxcl2*, *cxcl5*, *cxcl8*, *cxcl1*, *il1a*, and *il1b*. (B–G) Gene expression of the indicated genes in a second independent cohort from The Cancer Genome Atlas. Data are representative of 275 ADC and 349 control samples. (H) Deconvolution analysis of the same samples shows the proportions of different leukocytes found within normal and colon ADC samples. The black arrows denote the neutrophils in both groups (I). Neutrophil numbers are higher in tumors. *$P < 0.05$, ****$P < 0.0001$.

chemokine and inflammatory molecule transcripts were expressed by colon adenocarcinomas (ADC). Bioinformatical analysis of bulk RNA-seq of 342 colon ADC and 231 healthy samples revealed that chemokines such as *cxcl2*, *cxcl1*, *cxcl8*, and *cxcl5*, which are involved in neutrophil recruitment, were highly expressed in tumor tissue samples compared to control tissue (Fig. 1A). Also, *il1a* and *il1b*, known to be involved in chemokine production, were upregulated. A similar analysis in the GEPIA portal confirmed these results (Fig. 1B–G). By contrast, other chemokines not involved in neutrophil traffic, such as *ccl2*, *ccl11*, *ccl13*, *ccl14*, *ccl23*, and *cxcl12*, were found at lower levels in colon ADC samples compared to their healthy counterparts (Supplementary Fig. 1 A and B).

To correlate the presence of chemokine transcripts within colon ADC with the presence of TANs, we performed a deconvolution analysis of the same samples. According to the gene signatures, our analysis revealed that most types of leukocytes were present in both healthy and ADC colon tissues but at different frequencies (Fig. 1H). Further analysis of these data indicated that neutrophils were at higher proportions in colon ADC than healthy controls (Fig. 1I). Together, colon ADC samples produced many transcripts codifying for chemokines involved in the migration of neutrophils and other leukocytes, and neutrophils were predicted to be found at higher proportions in colon ADC compared to healthy colon tissues.

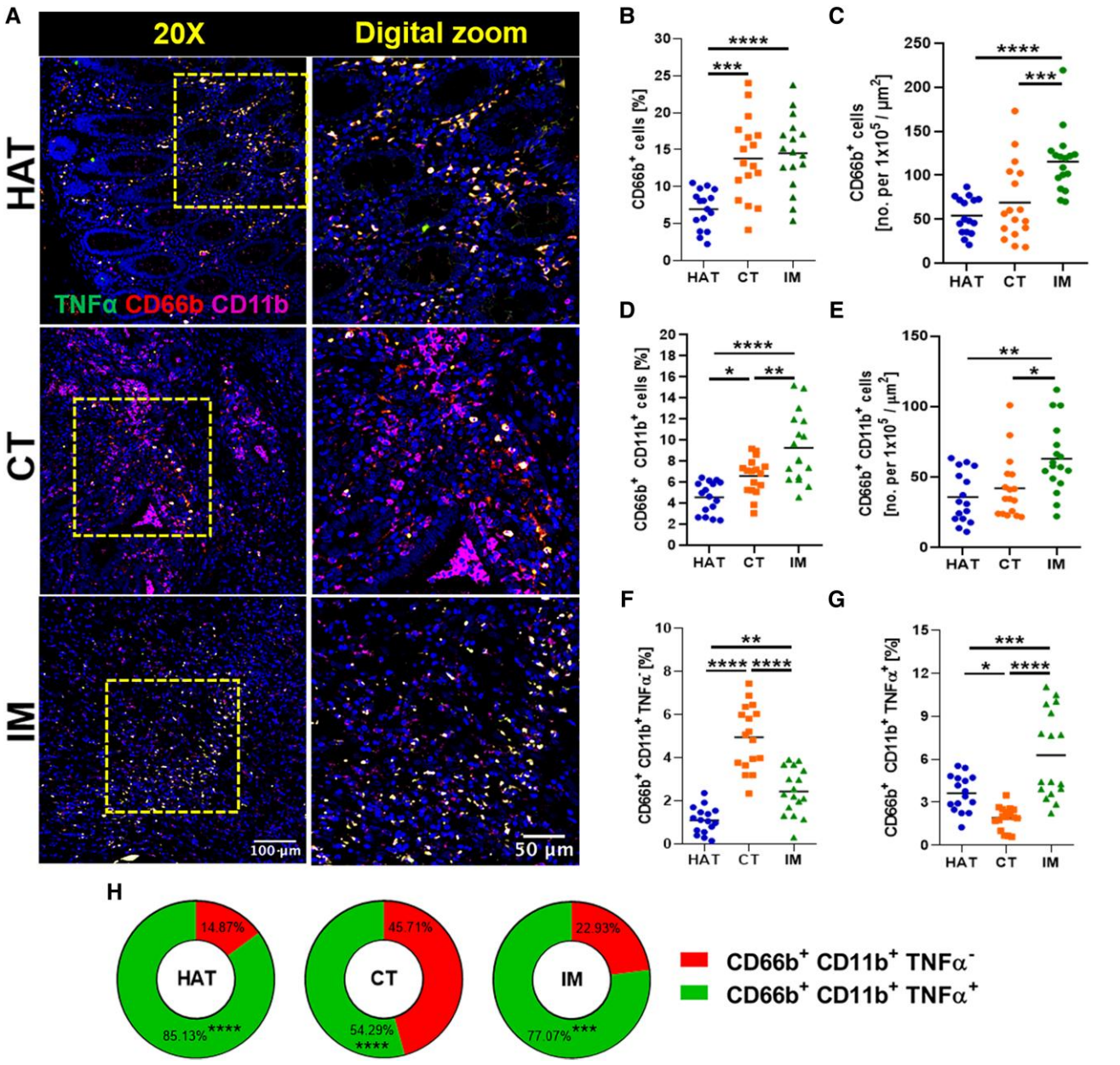


Fig. 2. TNFα$^+$ neutrophils are more represented at the IM of colon cancer samples than at the CT and HAT. (A) Representative images of HAT, CT, and IM of colon cancer tissues. The left panel represents images at a magnification of 20×. The right panel corresponds to a digital zoom of the area marked by the yellow square of the images of the left panel. The white bar on the left panel represents 100 µm. The white bar on the right panel represents 50 µm. DAPI is in blue, CD11b is in purple, and yellow corresponds to CD11b$^+$ CD66b$^+$ TNFα$^+$. Quantification of (B) frequency of CD66b$^+$ cells, (C) absolute numbers of CD66b$^+$ cells within $1 \times 10^5$ µm$^2$, (D) frequency of CD66b$^+$CD11b$^+$ cells, (E) absolute numbers of CD66b$^+$CD11b$^+$ cells within $1 \times 10^5$ µm$^2$, (F) frequency of CD66b$^+$CD11b$^+$TNFα$^-$ cells, and (G) frequency of CD66b$^+$CD11b$^+$TNFα$^+$ cells. (H) Frequency of neutrophils expressing TNFα in HAT, CT, and IM. Data are represented as mean ± SD of 16 patients per group. *$P < 0.05$, **$P < 0.01$, ***$P < 0.001$, ****$P < 0.0001$.

## 3.2 TNFα$^+$ neutrophils are more represented at the IM of colon cancer samples than at the CT and healthy adjacent tissues

To validate our bioinformatical analysis, we specifically investigated the presence of neutrophils in different tumor layers. Neutrophils were detected by the expression of CD66b and CD11b. Double-positive cells that additionally expressed TNFα were considered to have an antitumoral phenotype.[13] These triple-positive cells were more frequent in the IM than in the CT and HAT (Fig. 2A). Quantification revealed that CD66b$^+$ CD11b$^+$ cells were more abundant in frequency and absolute numbers at the CT and IM of the tumor when compared to HAT (Fig. 2B–E). TNFα$^-$ neutrophils were more frequent in the CT and IM portions of the tumor, while TNFα$^+$ neutrophils were more frequent in the IM (Fig. 2F–H). These results suggested neutrophils at the IM could have an antitumoral phenotype.

## 3.3 ICAM-1 and CD95 are more expressed in TANs than neutrophils in healthy adjacent tissues

To gain a better insight into the characteristics of colon cancer TANs, we performed multiparametric flow cytometry of the same portion of the samples analyzed by confocal microscopy.

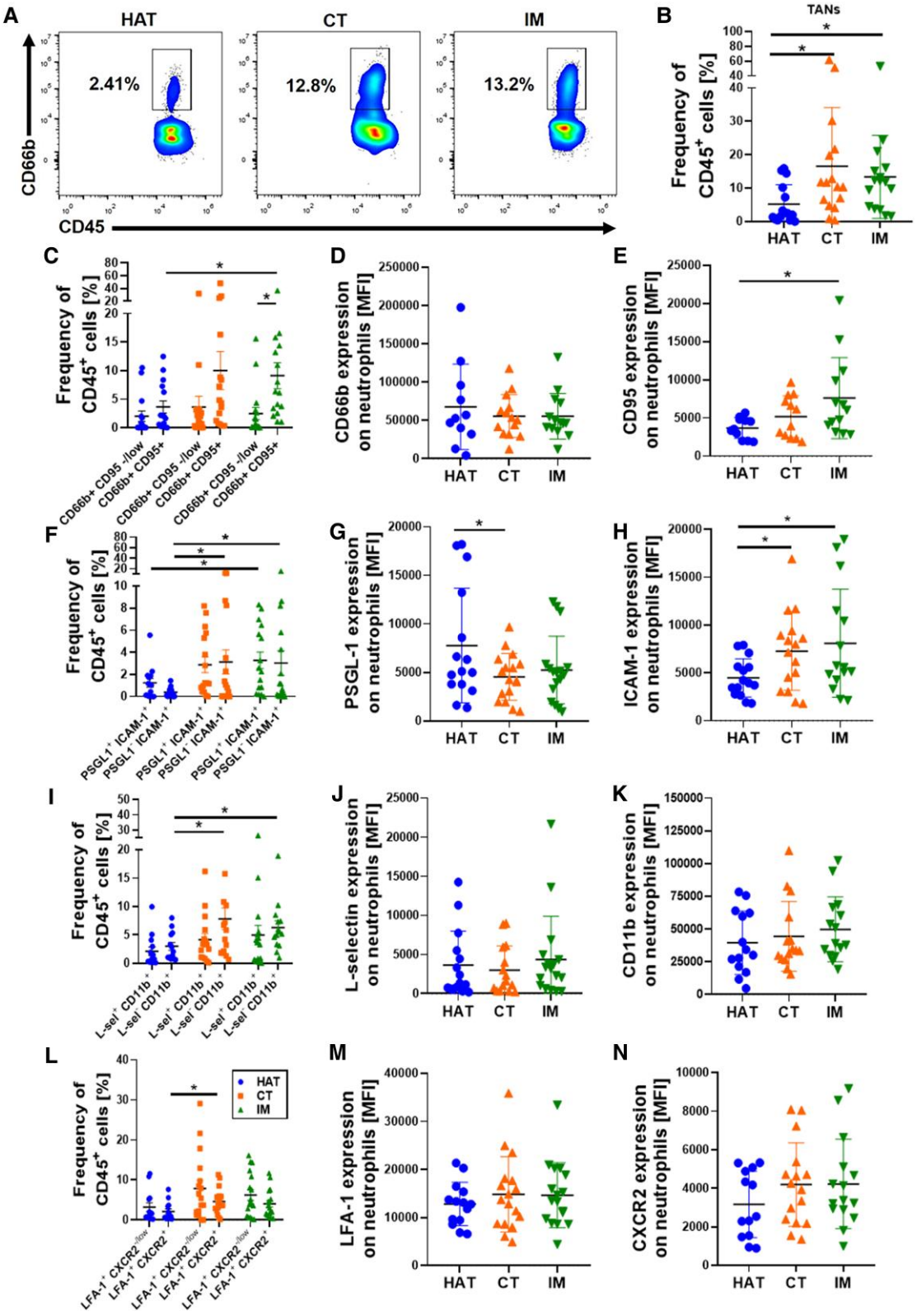


Fig. 3. ICAM-1 and CD95 are overexpressed in TANs compared to neutrophils in HAT. (A) Representative plots of the frequency of neutrophils with respect to total CD45$^+$ cells within HAT, colon cancer CT, and IM. (B) Frequency of neutrophils identified as CD45$^+$CD66b$^+$ cells. (C) Frequency of neutrophils expressing CD66b and CD95 at different tumor sections. Mean fluorescence intensity (MFI) of (D) CD66b and (E) CD95. (F) Frequency of neutrophils expressing PSGL-1 and ICAM-1 at different tumor sections. MFI of (G) PSGL-1 and (H) ICAM-1. (I) Frequency of neutrophils expressing L-selectin and CD11b at different tumor sections. MFI of (J) L-selectin and (K) CD11b. (L) Frequency of neutrophils expressing LFA-1 and CXCR2 at different tumor sections. MFI of (M) LFA-1 and (N) CXCR2. Data are represented as individual values mean ± SD of at least 15 patients per group. $^*P < 0.05$, $^{**}P < 0.01$.

These data confirmed that neutrophils are significantly more represented in the CT and the IM of the colon tumors than in HAT (Fig. 3A and B). $CD95^+$ neutrophils were more represented at the IM than in HAT; these cells were also found more frequently than $CD95^-$ neutrophils at the IM (Fig. 3C). The intensity of expression of CD66b on neutrophils did not show variations. In contrast, CD95 expression was more represented at the IM of colon tumors compared to HAT (Fig. 3D and E, respectively). ICAM-$1^+$ neutrophils were more represented at the IM and the CT when compared to HAT, while PSGL-1 expression on neutrophils showed a discrete but significant reduction at the CT, while ICAM-1 expression on neutrophils was more pronounced at the IM and the CT than in HAT (Fig. 3F–H). Neutrophils expressing CD11b and L-selectin were more represented at the IM and CT of colon tumors when compared to HAT. At the same time, no variations were recorded with respect to their expression (Fig. 3I–K). Moreover, our data show that $CXCR2^+$ neutrophils were found at the CT of the tumors; however, no changes in LFA-1 or CXCR2 expression were found (Fig. 3L–N). Thus, these data confirmed that neutrophils with higher CD95 and ICAM-1 expression are more frequent in colon cancer samples than in HAT.

### 3.4 Neutrophils with an antitumoral phenotype are found at the IM of early-stage colon cancer samples

The NLR is a measurement that correlates with cancer progression and prognosis.[34,35] We wanted to know if this measurement in peripheral blood (PB) correlates to the pathologic state and the presence of neutrophils within different areas and colon tumors. First, we evaluated the NLR in PB and correlated it to the pathologic stage of patients. As expected, higher NLR were found in more advanced stages of the disease (Fig. 4A). Statistical analysis of the data collected from patients together with previous reports[35] showed that an NLR of 3.5 may serve as a threshold to distinguish early stages (I/II) from late stages (III/IV) of colon cancer (Supplementary Table 1 and Supplementary Fig. 2). Surprisingly, when we correlated this threshold in PB to our flow cytometry data, we observed that TANs were more frequent in the CT and the IM when patients had an NLR $\leq$3.5 in PB (Fig. 4B–E). Pairing our flow cytometry data to the stage of the disease showed that CD95 (Fig. 4F and G) and ICAM-1 (Fig. 4H and I) were more expressed in neutrophils from the IM at the early stages compared to the late stages of the disease. Thus, our data suggest that neutrophils with an antitumoral phenotype are more frequent in the CT and IM of colon cancer samples of patients showing a PB NLR $\leq$3.5 and that neutrophils with the most marked antitumoral phenotype (high CD95 and ICAM-1 expression) are located preferentially in the IM of early-stage colon cancer samples.

### 3.5 Neutrophils are polarized to an antitumoral phenotype upon direct interaction with colon cancer cells

Finally, to verify if direct contact of neutrophils with colon cancer cells induces the expression of CD95 and ICAM-1, we performed in vitro cocultures of healthy donor-derived neutrophils with 2 different colon cancer cell lines. In line with data derived from colon cancer samples, we observed increased expression of CD95 (Fig. 5A and B) and ICAM-1 (Fig. 5C and D) in neutrophils in direct contact with colon cancer cells. Moreover, we also found augmented expression of CXCR2 (Fig. 5E and F). Other molecules such as CD62-L (Fig. 5G and H), CD66b (Fig. 5I and J), CD11b (Fig. 5K and L), LFA-1 (Fig. 5M and N), and PSGL-1 (Fig. 5O and P) did not show altered expression on neutrophils. Thus, our data suggest that increased CD95 and ICAM-1 expression is induced by the direct interaction of neutrophils with colon cancer cells.

## 4. Discussion

Most information concerning TANs comes from experimental mouse models that do not necessarily resemble human tissues. This information is fundamental for comprehending tumor biology but cannot be simply extrapolated to humans. One crucial issue is that experimental models often resemble the late stages of the disease because they are established with tumoral cell lines derived from advanced tumors that have adapted to the pressure exerted by the immune system. This could explain why TANs are generally described as protumoral.[36] The scarce evidence in humans regarding the phenotype and function of TANs prompted us to characterize TANs in the context of human colon cancer. Our first approach was to investigate which chemokines are produced in human colon cancer tissues. We found that the main neutrophil chemoattractants (*cxcl1*, *cxcl2*, *cxcl5*, and *cxcl8*) and *il1a/b*, which are involved in inducing the production of these chemokines,[37] were upregulated at the transcript level in tumor samples when compared to normal tissues. Our deconvolution analysis predicted that neutrophils are more frequent in neoplastic samples when comparing them vs normal tissues. These data agree with previous reports showing that polymorphonuclear cells within human colon cancer were predicted as part of the tumor's immune cell composition.[38,39] To confirm our in silico predictions, we evaluated TAN presence and TNFα expression by confocal microscopy of tumor samples. We found that neutrophils are located in similar proportions in the CT and the IM of colon cancer tumors compared to HAT. This finding is in line with previous reports showing similar proportions of neutrophils in different layers of colon cancer samples.[21,39] Also, our observations showed that TNFα-expressing neutrophils were more frequent in the IM than in the CT. It is well known that mouse and human neutrophils with a proinflammatory phenotype express TNFα.[11,13] Thus, TANs in the IM of colon cancer tumors express TNFα, which suggested an inflammatory phenotype and cytotoxic phenotype.[40] It is worth noting that TNFα-negative TANs were located in all layers of the tumor but with a preference for the CT. $TNF\alpha^-$ neutrophils are described in mice and humans as N2 or anti-inflammatory;[11,13] however, their role at the CT of colon tumors remains elusive.

Information regarding the phenotype of TANs in the context of colon cancer is scarce. Considering the transcriptomic profiling of mouse neutrophils and the phenotype of human neutrophils under polarizing conditions toward N1/N2 phenotypes,[11,13] we sought to understand better the phenotype of TANs within the different layers of the tumors and HAT. We corroborated by flow cytometry that TANs were more frequent in the CT and IM than the HAT. Apart from TNFα, Fas/CD95 was more expressed by TANs from the IM, whereas ICAM-1 was upregulated in CT and IM compared to their HAT counterparts. Neutrophils expressing CD95 recognize its ligand CD95L on endothelial cells inducing LFA-1 activation and consequent neutrophil recruitment to inflamed tissues.[41] This also occurs in a mouse neuroblastoma model, where neutrophils are attracted to the tumors due to CD95L ectopic expression on neuroblastoma cells. In this model, neutrophils induced inflammation, but tumor killing was performed by $CD8^+$ T cells.[42] In concordance, in mice models of lymphoma, hepatoma, and melanoma, ectopic expression of CD95L on tumor cells induced neutrophil

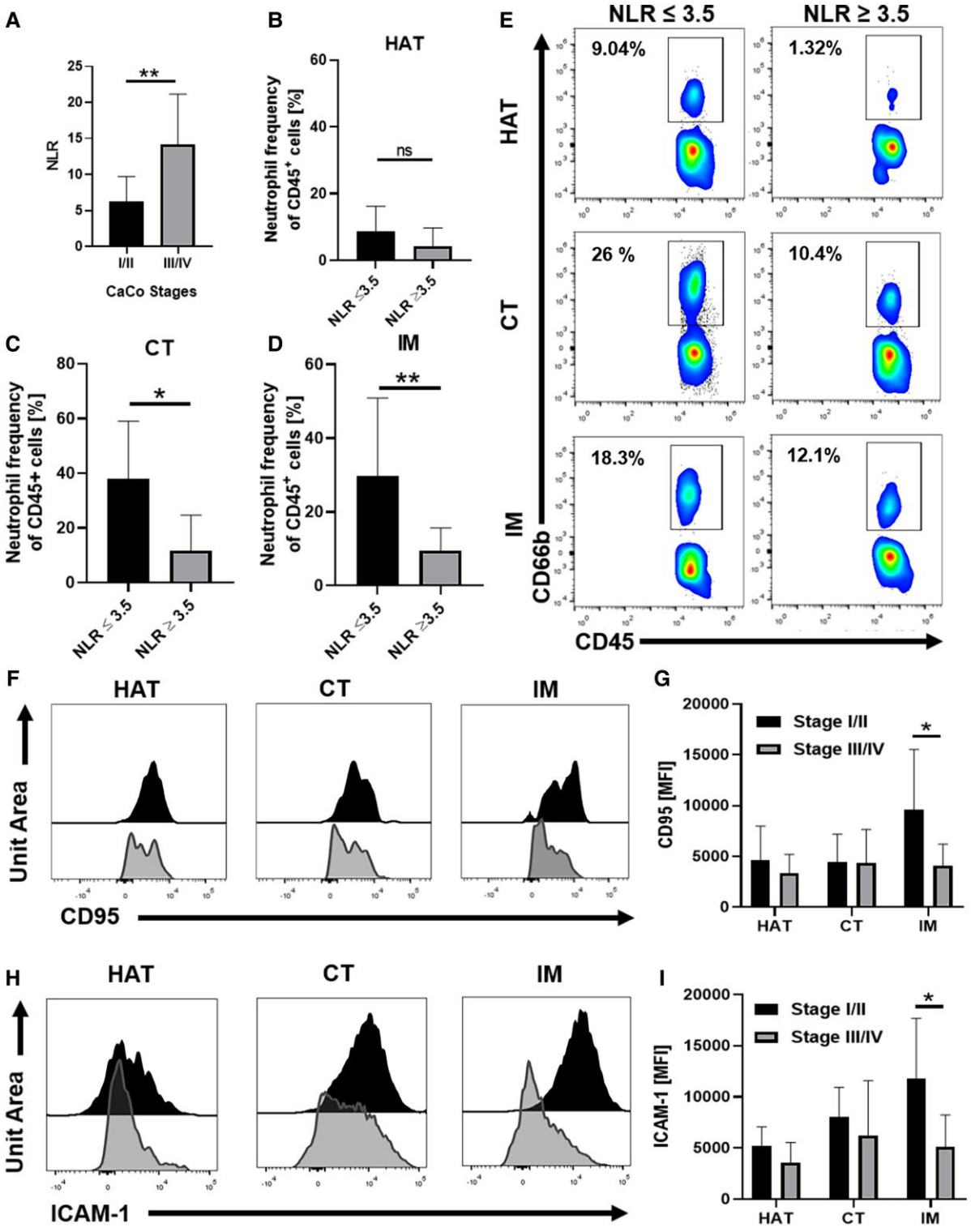


Fig. 4. Neutrophils with an antitumoral phenotype are found at the IM of early-stage colon cancer samples. (A) NLR in peripheral blood of patients grouped in early (I/II) ($n = 9$) and advanced stages (III/IV) ($n = 7$) of colon cancer. (B) Frequency of neutrophils in HAT, (C) CT, and (D) IM with respect to total CD45$^+$ cells within different layers of the tumor upon establishing a peripheral blood NLR threshold of 3.5. Results from NLR ≤3.5 are derived from 3 different samples. Results from NLR ≥3.5 are derived from 12 different samples. (E) Representative plots showing the frequency of neutrophils in the HAT, CT, and IM of colon cancer tumors employing the NLR threshold of 3.5. (F) Representative histograms showing the expression of CD95 on neutrophils from HAT, CT, and IM. (G) Quantification of CD95 MFI on neutrophils of different layers of the tumors and at different stages of the disease. (H) Representative histograms showing the expression of ICAM-1 on neutrophils from HAT, CT, and IM. (I) Quantification of ICAM-1 MFI on neutrophils of different layers of the tumors and at different stages of the disease. The black histograms correspond to stages I/II and the gray ones to stages III/IV. Data from early stages result from the mean of 9 different samples; data from stages III/IV are the result of the mean of 7 different samples. Data are represented as mean ± SD. *$P < 0.05$, **$P < 0.01$.

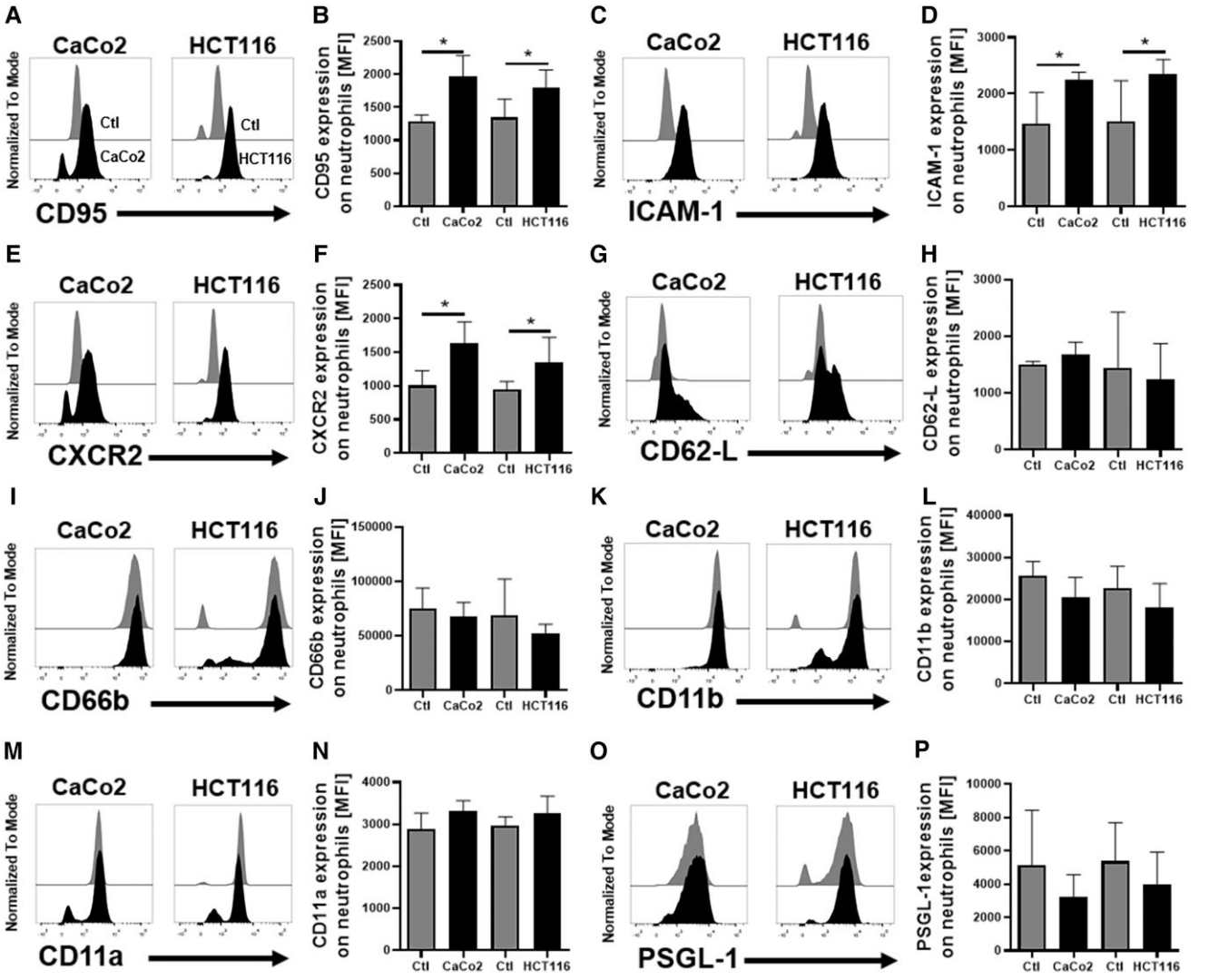


Fig. 5. Neutrophils are polarized toward an antitumoral phenotype upon direct interaction with colorectal cancer cell lines. (A) Representative histograms of CD95 expression on neutrophils cultured alone with culture media (gray histograms) or cocultured with CaCo2 or HCT116 cell lines (black histograms). (B) Quantification of CD95 MFI on neutrophils. (C, D) Representative histograms and quantification of ICAM-1 MFI on neutrophils. (E, F) Representative histograms and quantification of CXCR2 MFI on neutrophils. (G, H) Representative histograms and quantification of CD62-L MFI on neutrophils. (I, J) Representative histograms and quantification of CD66b MFI on neutrophils. (K, L) Representative histograms and quantification of CD11b MFI on neutrophils. (M, N) Representative histograms and quantification of CD11a MFI on neutrophils. (O, P) Representative histograms and quantification of PSGL-1 MFI on neutrophils. Data are represented as mean ± SD of at least 4 independent experiments. $^{*}P < 0.05$.

tumor killing in a CD95-dependent fashion.[43] In mice mesothelioma and lung models, CD95 is expressed at low levels; however, TGFβ receptor blocking enables neutrophils to express CD95 and their recruitment in vivo. These neutrophils exhibited direct cytotoxicity capabilities against tumoral cells in vitro.[12] Therefore, the direct antitumor activity of neutrophils in conjunction with the one exerted by $CD8^+$ T cells could be one of the reasons why their combined presence is associated with better prognosis in CRC.[44]

ICAM-1 is also upregulated by antitumoral neutrophils to participate in migration and as a stimulatory molecule upon activation.[22] These data and our confocal microscopy suggest that TANs in the IM possess an antitumoral phenotype, which suggests TANs could be combating tumor growth. Also, PSGL-1 was found to be significantly downregulated at the CT. PSGL-1 downregulation has been observed upon an inflammatory stimulus, which could suggest inflammation at the IM with the consequent induction of the antitumoral phenotype.[45] At early stages of lung cancer, human TANs display an activated phenotype marked by low expression of L-selectin and high ICAM-1 and CD95 expression compared to PB neutrophils. In the early stages of lung cancer, TANs were found to induce the proliferation of cytotoxic and helper T cells.[25] It will be interesting to know if TANs found in colon cancer can also stimulate T-cell responses, which could, at least in part, explain how TANs are acting in this context. Also, our findings are in line with this report as we found weak expression of L-selectin in our conditions at the different tumor layers, indicating neutrophil activation. IFNβ is used as a therapeutic agent in patients with melanoma as it is a potent antitumoral agent. In breast cancer and melanoma models, the administration of IFNβ augmented the ICAM-1, CD95, and TNFα expression on TANs, which suggested that the induction of an antitumoral phenotype in TANs should be of benefit in the treatment of diseases such as melanoma.[22] In our study, we found this phenotype which supports TANs at the IM possesses an antitumoral phenotype. As in other conditions such as sepsis[46,47] or acute kidney injury,[48] neutrophils are a "double-edged sword" that could be

detrimental when acting in an excessive fashion. In the context of cancer, for example, activated TNFα-producing neutrophils promote angiotropism of melanoma cells and metastasis.[49] We do not discard the possibility that antitumoral neutrophils could also promote colon cancer metastasis; this is an idea we are currently testing.

We correlated our experimental data with the patients' characteristics. High NLR correlates to a poor prognosis in colorectal, gastric, esophageal, pancreatic, lung, renal, and ovary cancers, among others.[50] Although our cohort of patients is relatively small, we observed significant differences in NLR among early and late stages of colon cancer. Surprisingly, applying an NLR threshold of 3.5, we observed that TANs were more represented in the CT and IM of colon cancer samples. We also observed that by stratifying our observations according to the pathologic stage, TANs at early stages possessed a more antitumoral phenotype, as characterized by a higher expression of CD95 and ICAM-1 at the IM. These observations might suggest that TANs at the early stages of colon cancer are more capable of combating colon cancer growth. In contrast, we observed TANs at the late stages of colon cancer had a less activated phenotype. This could suggest that the tumor has evolved at late stages and is more capable of modulating the immune responses to favor its development. An early study indicated that the high presence of neutrophils in CRC tissues correlates with worse survival after surgery in the early and late stages of the disease.[16] More recently, poor neutrophil infiltration at the invasive front in the early stages of colon cancer indicated poor prognosis of patients in terms of overall survival.[18] Moreover, poor infiltration of $CD66b^+$ cells at the IM showed a worse patient prognosis[18] and the high presence of myeloperoxidase (MPO)–positive cells within CRC samples correlated to better survival probability of patients.[17] In agreement, a high infiltration of $MPO^+$ cells in CRC is associated with a favorable prognosis. In contrast, samples with poor $MPO^+$ cell infiltrate were associated with poor prognosis.[51] It remains to be seen if patients with higher TANs at the IM that display an antitumoral phenotype can be associated with better prognosis.

In support of our patient-derived data, in vitro coculture of colon cancer cells and primary neutrophils also showed the induction of neutrophil activation marked by higher ICAM-1, CD95, and variations in CXCR2 expression. However, other molecules were not altered as in tumor samples, likely due to tumor factors that are not present in our cell culture conditions. These experiments prove that direct contact of colon cancer cells with neutrophils is sufficient to induce an antitumoral phenotype. In our understanding, this type of coculture has not been performed to study the neutrophil behavior in these conditions. Still, we believe it is a good, adaptable in vitro model to study the neutrophil–colon cancer cell interactions. It will be interesting to investigate in this in vitro model other factors known to alter the phenotype and function of TANs, for instance, hypoxia known to induce anti-inflammatory (N2) phenotypes.[11]

In summary, our observations suggest that TANs are more frequent in the IM of tumors of the early stages of colon cancer, where they possess an antitumoral phenotype. In addition to the presence of neutrophils, it will be interesting to know if the finding of an antitumoral phenotype in TANs would also correlate to better survival of patients with colon cancer.

## Acknowledgments

We thank Dr. Miguel Vargas, who kindly provided the cell lines employed in this project. This work was supported by the following grants: The National Strategic Program (Pronace) in Leukemias of the Mexican National Council for Science and Technology CONACyT, PRONACE Salud, PRONAII Leucemia, Project 302978 to M.S.; the program Ciencia de Fronteras CONACyT, Project 21887; Research Grant no. IMSS-R-785-063 supported by GL PRO—FUNDACIÓN IMSS A.C to H.M.; grants from CONACYT to R.P. (CB A1-S-30723 and PRONAII 302941); and grants awarded by the IMSS: CONACyT, PRONACE project 302962 to L.B. with IMSS registration number R-2020-785-004 and IMSS with registration number R-2022-785-048 to E.V.

## Author contributions

E.V. designed and supervised the study, performed experiments, analyzed, and interpreted data, performed statistical analyses, and wrote the manuscript. C.A.-F., S.G.D.L.-R., J.B., and C.F.-C. performed experiments, analyzed, and interpreted data, and performed statistical analyses. S.V.-P., K.T.-P., and D.M.-R. performed bioinformatical analysis. A.M. and L.R. provided pathologic analysis, selected patients included in the study, and performed statistical analysis. I.I.L.-V. interpreted data and helped write the manuscript draft. P.P.-S. performed histology and contributed to the study design. J.L.P.-C. and V.P.-K. designed and contributed to the study design. J.M.M., L.B., R.P., H.M., and M.S. helped in design and analysis and obtained the funding.

## Supplementary material

Supplementary materials are available at *Journal of Leukocyte Biology* online.

*Conflict of interest statement*. None declared.

## References

1. Siegel RL, Miller KD, Goding Sauer A, Fedewa SA, Butterly LF, Anderson JC, Cercek A, Smith RA, Jemal A. Colorectal cancer statistics, 2020. *CA Cancer J Clin*. 2020:70(3):145–164. https://doi.org/10.3322/caac.21601
2. Matsuda T, Yamashita K, Hasegawa H, Oshikiri T, Hosono M, Higashino N, Yamamoto M, Matsuda Y, Kanaji S, Nakamura T, *et al.* Recent updates in the surgical treatment of colorectal cancer. *Ann Gastroenterol Surg*. 2018:2(2):129–136. https://doi.org/10.1002/ags3.12061
3. Chakedis J, Schmidt CR. Surgical treatment of metastatic colorectal cancer. *Surg Oncol Clin N Am*. 2018:27(2):377–399. https://doi.org/10.1016/j.soc.2017.11.010
4. Jackstadt R, van Hooff SR, Leach JD, Cortes-Lavaud X, Lohuis JO, Ridgway RA, Wouters VM, Roper J, Kendall TJ, Roxburgh CS, *et al.* Epithelial NOTCH signaling rewires the tumor microenvironment of colorectal cancer to drive poor-prognosis subtypes and metastasis. *Cancer Cell*. 2019:36(3):319–336.e7. https://doi.org/10.1016/j.ccell.2019.08.003
5. Hiraki M, Tanaka T, Sadashima E, Sato H, Kitahara K. The clinical impact of apical lymph node metastasis of colorectal cancer after curative resection. *J Gastrointest Cancer*. 2022:54(2):506–512. https://doi.org/10.1007/S12029-022-00828-W
6. Tsilimigras DI, Brodt P, Clavien PA, Muschel RJ, D'Angelica MI, Endo I, Parks RW, Doyle M, de Santibañes E, Pawlik TM. Liver metastases. *Nat Rev Dis Prim*. 2021:7(1):27. https://doi.org/10.1038/S41572-021-00261-6
7. Chimal-Ramírez GK, Espinoza-Sanchez NA, Fuentes-Panana EM. A role for the inflammatory mediators cox-2 and metalloproteinases in cancer stemness. *Anticancer Agents Med Chem*. 2015:15(7):837–855. https://doi.org/10.2174/1871520615666150318100822

8. Galon J, Costes A, Sanchez-Cabo F, Kirilovsky A, Mlecnik B, Lagorce-Pagès C, Tosolini M, Camus M, Berger A, Wind P, *et al.* Type, density, and location of immune cells within human colorectal tumors predict clinical outcome. *Science*. 2006:313(5795):1960–1964. https://doi.org/10.1126/science.1129139
9. Xie X, Shi Q, Wu P, Zhang X, Kambara H, Su J, Yu H, Park SY, Guo R, Ren Q, *et al.* Single-cell transcriptome profiling reveals neutrophil heterogeneity in homeostasis and infection. *Nat Immunol*. 2020:21(9):1119–1133. https://doi.org/10.1038/s41590-020-0736-z
10. Chen S, Zhang Q, Lu L, Xu C, Li J, Zha J, Ma F, Luo HR, Hsu AY. Heterogeneity of neutrophils in cancer: one size does not fit all. *Cancer Biol Med*. 2022:19(12):1629–1648. https://doi.org/10.20892/j.issn.2095-3941.2022.0426
11. Ohms M, Möller S, Laskay T. An attempt to polarize human neutrophils toward N1 and N2 phenotypes in vitro. *Front Immunol*. 2020:11:532. https://doi.org/10.3389/FIMMU.2020.00532
12. Fridlender ZG, Sun J, Kim S, Kapoor V, Cheng G, Ling L, Worthen GS, Albelda SM. Polarization of tumor-associated neutrophil phenotype by TGF-beta: "N1" versus "N2" TAN. *Cancer Cell*. 2009:16(3):183–194. https://doi.org/10.1016/j.ccr.2009.06.017
13. Mihaila AC, Ciortan L, Macarie RD, Vadana M, Cecoltan S, Preda MB, Hudita A, Gan AM, Jakobsson G, Tucureanu MM, *et al.* Transcriptional profiling and functional analysis of N1/N2 neutrophils reveal an immunomodulatory effect of S100A9-blockade on the pro-inflammatory N1 subpopulation. *Front Immunol*. 2021:12:708770. https://doi.org/10.3389/FIMMU.2021.708770
14. van Vlerken-Ysla L, Tyurina YY, Kagan VE, Gabrilovich DI. Functional states of myeloid cells in cancer. *Cancer Cell*. 2023:41(3):490–504. https://doi.org/10.1016/j.ccell.2023.02.009
15. Quail DF, Amulic B, Aziz M, Barnes BJ, Eruslanov E, Fridlender ZG, Goodridge HS, Granot Z, Hidalgo A, Huttenlocher A, *et al.* Neutrophil phenotypes and functions in cancer: a consensus statement. *J Exp Med*. 2022:219(6):e20220011. https://doi.org/10.1084/JEM.20220011
16. Rao HL, Chen JW, Li M, Xiao YB, Fu J, Zeng YX, Cai MY, Xie D. Increased intratumoral neutrophil in colorectal carcinomas correlates closely with malignant phenotype and predicts patients' Adverse prognosis. *PLoS One*. 2012:7(1):e30806. https://doi.org/10.1371/JOURNAL.PONE.0030806
17. Droeser RA, Hirt C, Eppenberger-Castori S, Zlobec I, Viehl CT, Frey DM, Nebiker CA, Rosso R, Zuber M, Amicarella F, *et al.* High myeloperoxidase positive cell infiltration in colorectal cancer is an independent favorable prognostic factor. *PLoS One*. 2013:8(5):e64814. https://doi.org/10.1371/JOURNAL.PONE.0064814
18. Wikberg ML, Ling A, Li X, Öberg Å, Edin S, Palmqvist R. Neutrophil infiltration is a favorable prognostic factor in early stages of colon cancer. *Hum Pathol*. 2017:68:193–202. https://doi.org/10.1016/j.humpath.2017.08.028
19. Yang L, Liu Q, Zhang X, Liu X, Zhou B, Chen J, Huang D, Li J, Li H, Chen F, *et al.* DNA Of neutrophil extracellular traps promotes cancer metastasis via CCDC25. *Nature*. 2020:583(7814):133–138. https://doi.org/10.1038/s41586-020-2394-6
20. Chandra R, Karalis JD, Liu C, Murimwa GZ, Park JV, Heid CA, Reznik SI, Huang E, Minna JD, Brekken RA. The colorectal cancer tumor microenvironment and its impact on liver and lung metastasis. *Cancers (Basel)*. 2021:13(24):6206. https://doi.org/10.3390/cancers13246206
21. Mezheyeuski A, Micke P, Martín-bernabé A, Backman M, Hrynchyk I, Hammarström K, Ström S, Ekström J, Edqvist PH, Sundström M, *et al.* The immune landscape of colorectal cancer. *Cancers (Basel)*. 2021:13(21):5545. https://doi.org/10.3390/CANCERS13215545
22. Andzinski L, Kasnitz N, Stahnke S, Wu CF, Gereke M, Von Köckritz-Blickwede M, Schilling B, Brandau S, Weiss S, Jablonska J. Type I IFNs induce anti-tumor polarization of tumor associated neutrophils in mice and human. *Int J Cancer*. 2016:138(8):1982–1993. https://doi.org/10.1002/ijc.29945
23. Jablonska J, Leschner S, Westphal K, Lienenklaus S, Weiss S. Neutrophils responsive to endogenous IFN-beta regulate tumor angiogenesis and growth in a mouse tumor model. *J Clin Invest*. 2010:120(4):1151–1164. https://doi.org/10.1172/JCI37223
24. Houghton AMG, Rzymkiewicz DM, Ji H, Gregory AD, Egea EE, Metz HE, Stolz DB, Land SR, Marconcini LA, Kliment CR, *et al.* Neutrophil elastase-mediated degradation of IRS-1 accelerates lung tumor growth. *Nat Med*. 2010:16(2):219–223. https://doi.org/10.1038/nm.2084
25. Eruslanov EB, Bhojnagarwala PS, Quatromoni JG, Stephen TL, Ranganathan A, Deshpande C, Akimova T, Vachani A, Litzky L, Hancock WW, *et al.* Tumor-associated neutrophils stimulate T cell responses in early-stage human lung cancer. *J Clin Invest*. 2014:124(12):5466–5480. https://doi.org/10.1172/JCI77053
26. Galdiero MR, Varricchi G, Loffredo S, Mantovani A, Marone G. Roles of neutrophils in cancer growth and progression. *J Leukoc Biol*. 2018:103(3):457–464. https://doi.org/10.1002/JLB.3MR0717-292R
27. Tang Z, Li C, Kang B, Gao G, Li C, Zhang Z. GEPIA: a web server for cancer and normal gene expression profiling and interactive analyses. *Nucleic Acids Res*. 2017:45(W1):W98–W102. https://doi.org/10.1093/nar/gkx247
28. Tang Z, Kang B, Li C, Chen T, Zhang Z. GEPIA2: an enhanced web server for large-scale expression profiling and interactive analysis. *Nucleic Acids Res*. 2019:47(W1):W556–W560. https://doi.org/10.1093/nar/gkz430
29. Aran D, Camarda R, Odegaard J, Paik H, Oskotsky B, Krings G, Goga A, Sirota M, Butte AJ. Comprehensive analysis of normal adjacent to tumor transcriptomes. *Nat Commun*. 2017:8(1):1077. https://doi.org/10.1038/s41467-017-01027-z
30. De León Rodríguez SG, Hernández Herrera P, Aguilar Flores C, Pérez Koldenkova V, Guerrero A, Mantilla A, Fuentes-Pananá EM, Wood C, Bonifaz LC. A machine learning workflow of multiplexed immunofluorescence images to interrogate activator and tolerogenic profiles of conventional type 1 dendritic cells infiltrating melanomas of disease-free and metastatic patients. *J Oncol*. 2022:2022:9775736. https://doi.org/10.1155/2022/9775736
31. Stringer C, Wang T, Michaelos M, Pachitariu M. Cellpose: a generalist algorithm for cellular segmentation. *Nat Methods*. 2021:18(1):100–106. https://doi.org/10.1038/s41592-020-01018-x
32. Pécot T, Cuitiño MC, Johnson RH, Timmers C, Leone G. Deep learning tools and modeling to estimate the temporal expression of cell cycle proteins from 2D still images. *PLoS Comput Biol*. 2022:18(3):e1009949. https://doi.org/10.1371/JOURNAL.PCBI.1009949
33. Espinoza-Sánchez NA, Chimal-Ramírez GK, Mantilla A, Fuentes-Pananá EM. IL-1, IL-8, and matrix metalloproteinases-1, -2, and -10 are enriched upon monocyte-breast cancer cell cocultivation in a matrigel-based three-dimensional system. *Front Immunol*. 2017:8:205. https://doi.org/10.3389/fimmu.2017.00205
34. Cupp MA, Cariolou M, Tzoulaki I, Aune D, Evangelou E, Berlanga-Taylor AJ. Neutrophil to lymphocyte ratio and cancer prognosis: an umbrella review of systematic reviews and meta-analyses of observational studies. *BMC Med*. 2020:18(1):360. https://doi.org/10.1186/S12916-020-01817-1
35. Howard R, Kanetsky PA, Egan KM. Exploring the prognostic value of the neutrophil-to-lymphocyte ratio in cancer. *Sci Rep*. 2019:9(1):19673. https://doi.org/10.1038/s41598-019-56218-z
36. Eruslanov EB, Singhal S, Albelda SM. Mouse versus human neutrophils in cancer: a major knowledge gap. *Trends Cancer*. 2017:3(2):149–160. https://doi.org/10.1016/j.trecan.2016.12.006

37. Pyrillou K, Burzynski LC, Clarke MCH. Alternative pathways of IL-1 activation, and its role in health and disease. *Front Immunol*. 2020:11:613170. https://doi.org/10.3389/FIMMU.2020.613170
38. Gentles AJ, Newman AM, Liu CL, Bratman SV, Feng W, Kim D, Nair VS, Xu Y, Khuong A, Hoang CD, *et al*. The prognostic landscape of genes and infiltrating immune cells across human cancers. *Nat Med*. 2015:21(8):938–945. https://doi.org/10.1038/nm.3909
39. Bindea G, Mlecnik B, Tosolini M, Kirilovsky A, Waldner M, Obenauf AC, Angell H, Fredriksen T, Lafontaine L, Berger A, *et al*. Spatiotemporal dynamics of intratumoral immune cells reveal the immune landscape in human cancer. *Immunity*. 2013:39(4): 782–795. https://doi.org/10.1016/j.immuni.2013.10.003
40. Mishalian I, Bayuh R, Levy L, Zolotarov L, Michaeli J, Fridlender ZG. Tumor-associated neutrophils (TAN) develop pro-tumorigenic properties during tumor progression. *Cancer Immunol Immunother*. 2013:62(11):1745–1756. https://doi.org/10.1007/s00262-013-1476-9
41. Gao L, Gülcüler GS, Golbach L, Block H, Zarbock A, Martin-Villalba A. Endothelial cell-derived CD95 ligand serves as a chemokine in induction of neutrophil slow rolling and adhesion. *Elife*. 2016:5:e18542. https://doi.org/10.7554/ELIFE.18542
42. Shimizu M, Fontana A, Takeda Y, Yagita H, Yoshimoto T, Matsuzawa A. Induction of antitumor immunity with fas/APO-1 ligand (CD95L)-transfected neuroblastoma neuro-2a cells. *J Immunol*. 1999:162(12):7350–7357. https://doi.org/10.4049/jimmunol.162.12.7350
43. Seino KI, Kayagaki N, Okumura KO, Yagita H. Antitumor effect of locally produced CD95 ligand. *Nat Med*. 1997:3(2):165–170. https://doi.org/10.1038/nm0297-165
44. Chengzeng YIN, Okugawa Y, Yamamoto A, Kitajima T, Shimura T, Kawamura M, Tsujiura M, Okita Y, Masaki OHI, Toiyama Y. Prognostic significance of CD8+ tumor-infiltrating lymphocytes and CD66b+ tumor-associated neutrophils in the invasive margins of stages I-III colorectal cancer. *Oncol Lett*. 2022:24(1):212. https://doi.org/10.3892/OL.2022.13333
45. Marsik C, Mayr F, Cardona F, Schaller G, Wagner OF, Jilma B. Endotoxin down-modulates P-selectin glycoprotein ligand-1 (PSGL-1, CD162) on neutrophils in humans. *J Clin Immunol*. 2004:24(1): 62–65. https://doi.org/10.1023/B:JOCI.0000018064.13793.83
46. Guerrero-Fonseca IM, García-Ponce A, Vadillo E, Lartey NL, Vargas-Robles H, Chánez-Paredes S, Castellanos-Martínez R, Nava P, Betanzos A, Neumann BM, *et al*. HS1 Deficiency protects against sepsis by attenuating neutrophil-inflicted lung damage. *Eur J Cell Biol*. 2022:101(2):51214. https://doi.org/10.1016/J.EJCB.2022.151214
47. Schnoor M, García Ponce A, Vadillo E, Pelayo R, Rossaint J, Zarbock A. Actin dynamics in the regulation of endothelial barrier functions and neutrophil recruitment during endotoxemia and sepsis. *Cell Mol Life Sci*. 2017:74(11):1985–1997. https://doi.org/10.1007/s00018-016-2449-x
48. Margraf A, Cappenberg A, Vadillo E, Ludwig N, Thomas K, Körner K, Zondler L, Rossaint J, Germena G, Hirsch E, *et al*. ArhGAP15, a RacGAP, acts as a temporal signaling regulator of mac-1 affinity in sterile inflammation. *J Immunol*. 2020:205(5):1365–1375. https://doi.org/10.4049/jimmunol.2000047
49. Bald T, Quast T, Landsberg J, Rogava M, Glodde N, Lopez-Ramos D, Kohlmeyer J, Riesenberg S, van den Boorn-Konijnenberg D, Hömig-Hölzel C, *et al*. Ultraviolet-radiation-induced inflammation promotes angiotropism and metastasis in melanoma. *Nature*. 2014:507(7490):109–113. https://doi.org/10.1038/nature13111
50. Guthrie GJK, Charles KA, Roxburgh CSD, Horgan PG, McMillan DC, Clarke SJ. The systemic inflammation-based neutrophil-lymphocyte ratio: experience in patients with cancer. *Crit Rev Oncol Hematol*. 2013:88(1):218–230. https://doi.org/10.1016/j.critrevonc.2013.03.010
51. Däster S, Eppenberger-Castori S, Hirt C, Soysal SD, Delko T, Nebiker CA, Weixler B, Amicarella F, Iezzi G, Governa V, *et al*. Absence of myeloperoxidase and CD8 positive cells in colorectal cancer infiltrates identifies patients with severe prognosis. *Oncoimmunology*. 2015:4(12):e1050574. https://doi.org/101080/2162402X20151050574